Spin Noise Spectroscopy in GaAs (110) Quantum Wells: Access to Intrinsic Spin Lifetimes and Equilibrium Electron Dynamics

Georg M. Müller,[1,*] Michael Römer,[1] Dieter Schuh,[2] Werner Wegscheider,[2] Jens Hübner,[1] and Michael Oestreich[1]

[1]*Institut für Festkörperphysik, Leibniz Universität Hannover, Appelstraße 2, 30167 Hannover, Germany*
[2]*Institut für Experimentelle und Angewandte Physik, Universität Regensburg, 93040 Regensburg, Germany*
(Received 11 September 2008; published 11 November 2008)

In this Letter, the first spin noise spectroscopy measurements in semiconductor systems of reduced effective dimensionality are reported. The nondemolition measurement technique gives access to the otherwise concealed intrinsic, low temperature electron spin relaxation time of *n*-doped GaAs (110) quantum wells and to the corresponding low temperature anisotropic spin relaxation. The Brownian motion of the electrons within the spin noise probe laser spot becomes manifest in a modification of the spin noise line width. Thereby, the spatially resolved observation of the stochastic spin polarization uniquely allows to study electron dynamics at equilibrium conditions with a vanishing total momentum of the electron system.

The dream of spin quantum information processing and spin based optoelectronic devices drives the current intense research on spin physics in semiconductors. Especially GaAs quantum wells (QW) with their quantization axis oriented in (110)-direction attract great attention since the electron spin relaxation times in these structures are extremely long even at room temperature. In bulk semiconductors with zinc blende structure, like GaAs, the spin dephasing of electrons is dominated over a wide temperature and doping range by the Dyakonov-Perel (DP) mechanism [1]: The lack of crystal inversion symmetry leads to a precession of the electron spin in the wave vector dependent Dresselhaus field $\mathbf{\Omega}(\mathbf{k})$ [2]. In (110) oriented GaAs QWs, the in-plane components of $\mathbf{\Omega}(\mathbf{k})$ vanish to all orders in the quasi momentum due to the special crystallographic symmetry and the quantum confinement in growth direction [3]. Thereby, the lifetime τ_z of electron spins aligned in growth direction of the (110) QW is considerably larger than in a (100) QW as experimentally shown first by Ohno *et al.* [4]. The spin relaxation time is not infinite but limited at high temperatures by intersubband electron scattering induced spin relaxation (ISR) [5]. At low temperatures, the efficiency of ISR is negligible but the well-known Bir Aronov Pikus (BAP) mechanism obviates in nearly all photoluminescence (PL) based experiments the observation of long τ_z. The BAP mechanism is caused by the spin interaction of the photo-created holes with the electrons in the conduction band which increases with decreasing temperature. The BAP mechanism can be avoided in (110) QWs by spatially separating electron and holes by surface acoustic waves [6]. However, the influence of the surface acoustic waves on τ_z is not clear yet. In other words, the intrinsic, undisturbed τ_z at low temperatures is unknown in (110) QWs.

In this Letter, we will show that the intrinsic, low temperature τ_z in modulation *n*-doped GaAs (110) QWs can be measured by the nondemolition measurement technique of spin noise spectroscopy and that the intrinsic τ_z is by more than 1 order of magnitude longer than measured by Ohno *et al.* [4] and Döhrmann *et al.* [5] by time-resolved PL. Spin noise spectroscopy (SNS) is a measurement technique known in quantum optics [7] and has been transferred to semiconductor systems just recently [8,9]. In SNS, the statistical fluctuations of the spin polarization are mapped via Faraday rotation onto the light polarization of a linear polarized, continuous-wave laser. The temporal dynamics of the spin fluctuations are characterized by the electron spin lifetime τ and, additionally, in the case of a magnetic field in Voigt geometry, by the precessional frequency ω. In the frequency domain, these temporal spin fluctuations translate to a Lorentzian line shape centered at $\omega/2\pi$ with a full width at half maximum of $1/\pi\tau$ [9,10]. In SNS experiments, the energy of the probing laser light is usually chosen to lie well below the energy gap where excitation of the semiconductor system is negligible [9]. Therefore, SNS allows experimental access to the electron spin dynamics near equilibrium without evoking parasitic spin relaxation by BAP.

The light source for the SNS measurements is a low noise, tunable diode laser in Littman configuration. A Faraday isolator avoids disturbing feedback and a spatial filter ensures a Gaussian beam profile. The laser light is focused to a beam waist of $w_0 \approx 3.5$ μm on the sample which is mounted in a He cold finger cryostat. Magnetic fields up to $\mu_0 H_{\text{ext}} = 14$ mT can be applied in Voigt geometry. The rotation of the linear light polarization is resolved by a combination of a polarizing beam splitter and a high bandwidth balanced photo receiver. The detected electrical signal is amplified by a low noise amplifier (40 dB) and sent through a low pass filter (-3 dB at 67 MHz). The fluctuation signal is digitized with 180 MHz in the time domain and Fourier transformed in real time.

In previous SNS measurements on bulk GaAs, the spin noise signal is shifted from zero frequency by applying a magnetic field in Voigt geometry. In (110)-oriented GaAs QWs, this method becomes difficult since spin relaxation is dominated in (110) QWs at finite magnetic fields by the DP dominated spin relaxation of the in-plane spin component. Therefore, small applied magnetic fields in Voigt geometry only lead to a broadening and, consequently, the spin noise spectra in this work are all centered around zero frequency. For the majority of spectra, large spurious background noise is most reliably removed by a double difference method: (a) The polarization of the laser light is switched between linear and circular polarization by a motorized Soleil Babinet compensator in front of the sample. Circular polarized light is not sensitive to changes in the Faraday rotation angle and, therefore, contains no spin noise information. (b) For each polarization the applied magnetic field is changed between $\mu_0 H_{\mathrm{ext}} = 14$ mT, at which the spin noise power becomes negligible in the observed frequency span, and zero or small magnetic fields. Subsequently, the noise power spectra for linear and circular polarized light are subtracted from each other, once for the applied magnetic field of $\mu_0 H_{\mathrm{ext}} = 14$ mT and once for a vanishing or smaller magnetic field. These two curves are on their part again subtracted from each other and the result is divided by a background noise spectrum to account for frequency dependent amplification.

The investigated sample consists of ten identical, symmetrically grown, nominally 16.8 nm thick GaAs QWs separated by 80 nm $Al_{0.39}Ga_{0.61}As$ barriers grown by molecular beam epitaxy and separated from the undoped (110) GaAs substrate by a 150 nm $Al_{0.80}Ga_{0.2}As$ lift-off sacrifice layer. The QWs are symmetrically modulation doped by Si δ-layers in the middle of the barriers and transport measurements under illumination yield a doping sheet density of $n = 1.8 \times 10^{11}$ cm^{-2} at 1.5 K. Photogalvanic experiments by Belkov *et al.* [11] have shown that spin dephasing due to structure inversion asymmetry is minimal in such symmetrically doped (110) QWs in contrast to symmetrically doped (100) QWs. The substrate is removed for the transmission SNS measurements following the lift-off recipe of Yablonovitch *et al.* [12], and the multi QW layer is van der Waals bonded to a c-cut sapphire substrate. White light transmission measurements identify the optical absorption edge (interband transition to the Fermi level energy) of the QWs between 813 and 814 nm.

The inset of Fig. 1 shows a typical SNS spectrum measured at a laser wavelength of 814.25 nm and a temperature of 20 K. The measured spin noise spectra are fitted with a Lorentz function centered at zero frequency. The area under the Lorentz curve gives the integrated spin noise power and the width determines the spin lifetime or spin decay rate γ, respectively. Figure 1 shows both the measured integrated spin noise power (black dots) and the spin relaxation rate (blue triangles) in dependence on laser wavelength for a lattice temperature of 20 K. The spin relaxation rate increases sharply when the laser wavelength
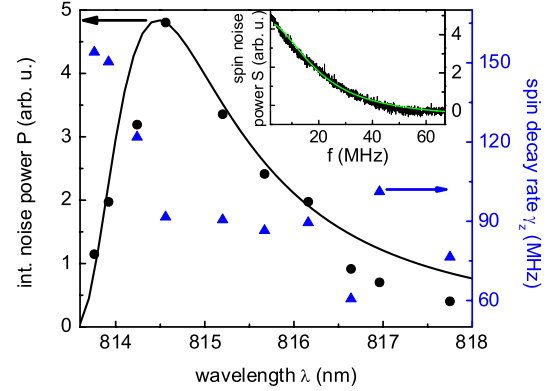

FIG. 1 (color online).   Spin decay rate $\gamma_z = 1/\tau_z$ and relative integrated spin noise power at $T = 20$ K as a function of the laser wavelength. Solid line: Integrated spin noise power according to model [9] (details in text). The inset shows a typical spin noise spectrum.

approaches the optical absorption edge. This observation is consistent with the fact that in this temperature regime traditional spin dephasing measurements based on optical excitation yield results which are completely obstructed by the BAP mechanism. Measurements of this increase of γ_z by SNS for wavelengths shorter than 813.7 nm are hindered by the fact that the integrated spin noise power approaches zero at the optical absorption edge and by the fixed frequency bandwidth of the detection setup. For wavelengths longer than 815 nm, optical absorption becomes negligible and the measured spin decay rate is in good approximation constant indicating that the residual spin life time is determined by other spin relaxation mechanisms than BAP. Further experiments presented below show that this spin decay rate is not yet the intrinsic spin relaxation time but limited by time of flight broadening.

The black dots and the solid black line in Fig. 1 depict the measured and the calculated integrated spin noise power, respectively. The integrated spin noise power P is calculated by a model which is based on the change of the refractive index due to the fluctuating imbalance of electron spins at the Fermi energy [9]: $P \propto \left[\frac{\partial n}{\partial \alpha}\big|_{\alpha_0} N_{\mathrm{fluc}}/N_{\mathrm{bleach}} \alpha_0\right]^2$, where n is the real part of the refractive index, N_{fluc} the root mean square imbalance between the two spin directions, N_{bleach} the critical imbalance that would bleach the optical transition for one spin direction, and α the absorption constant. The transition is set to 813.5 nm in accordance with the optical transmission measurements. The calculated wavelength dependence with the minimum of P at the optical absorption edge agrees well with the experimental data. Figure 2 shows a more detailed comparison of the measured and calculated P in dependence on temperature and wavelength. The following sample parameters are used for the calculation: The polarizability due to the optical selection rules of the optical transition is set to $\beta = 0.6$ [13] and an optical absorption constant $\alpha_0 = 2.28 \times 10^6$ m^{-1} is assumed
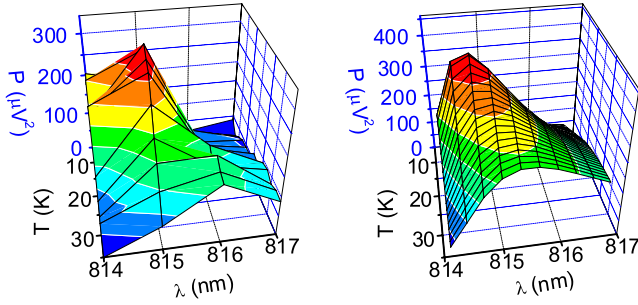
FIG. 2 (color online).   Absolute integrated spin noise power as a function of laser wavelength and temperature, measured (left panel) and calculated (right panel, details in text).

[14]. A line width of the optical resonance of $k_B \times 20$ K for $T \le 20$ K and of $k_B T$ for $T > 20$ K is used within the calculations since the width of the measured white light transmission change is constant below 20 K and increases linearly above. The energy of the resonance shifts with the temperature dependent Fermi level energy. Also this two-dimensional dependence of the calculated SNS on wavelength and temperature is in good agreement with our measurements, demonstrating that the origin of the spin noise signal is well understood.

Next, we observe the influence of the spin relaxation anisotropy on the spin noise signal, which has previously been examined at relatively high magnetic fields [5], where the spin relaxation anisotropy slows down the effective Larmor frequency. However, for very small magnetic fields, with $\omega_L < (\gamma_\perp - \gamma_z)/2$, there is no precessional motion of the spins as the spin decays due to the large in-plane spin relaxation rate $\gamma_\perp$ before a full rotation is carried out. The effective spin relaxation rate is in this case

$$\gamma_{\text{eff}} = \frac{\gamma_\perp + \gamma_z}{2} - \frac{\gamma_\perp - \gamma_z}{2}\sqrt{1 - 4\frac{\omega_L^2}{(\gamma_\perp - \gamma_z)^2}}. \quad (1)$$

Figure 3 depicts the measured γ_{eff} (black squares) as a function of applied magnetic field at $T = 20$ K. We have measured ω_L, i.e., an electron g factor $g^* = 0.29$, on the same sample by time-resolved PL at $B = 4$ T and fitted the spin noise data by a least square fit corresponding to Eq. (1) (top solid curve). The fit directly yields the anisotropy factor $\eta = \gamma_\perp/\gamma_z$ which is shown as filled squares in the inset of Fig. 3 in dependence on the laser wavelength. The anisotropy factor is smaller at 815 nm than at longer wavelengths since BAP is in contrast to DP at most weakly dependent on the crystallographic direction, i.e., an efficient isotropic spin relaxation lowers the spin relaxation anisotropy. In agreement with the wavelength dependent data (Fig. 1), the anisotropy factor is constant for long wavelengths since BAP is switched off.

Anisotropy measurements at 815 nm with a defocused, i.e., enlarged, laser spot on the sample reduce the spin relaxation by BAP and yield an anisotropy factor $\eta = 7.4(1.0)$ which is almost by a factor of 2 larger than in the focused case. This anisotropy factor is of the same
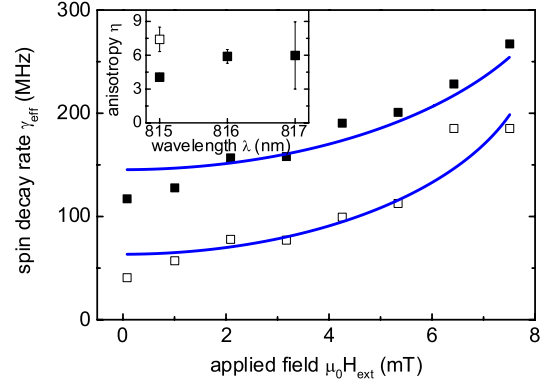

FIG. 3 (color online).   Effective spin decay rate $\gamma_{\text{eff}} = 1/\tau_{\text{eff}}$ ($T = 20$ K) as a function of the applied magnetic field with fits according to Eq. (1). Inset: Anisotropy determined by the fits as function of laser wavelength ($T = 20$ K). Open symbols indicate measurements with an enlarged laser spot in which time of flight broadening is strongly reduced.

magnitude as η measured in a similar sample at room temperature [5] and in an undoped GaAs (110) QW at low temperature [6]. However, the physical origins are different. In the room temperature case, the anisotropy is limited by ISR and, in the latter case, the anisotropy is probably dominated by the yet unclear influence of the surface acoustic waves. As it will be argued later in this Letter, the anisotropy measured in this work is in contrast given by the intrinsic low temperature spin lifetimes of the sample. Still, the strong measured increase of τ_z after defocusing cannot be solely explained by the reduction of BAP since η is only equal to about 6 for laser wavelengths of 816 and 817 nm where BAP is negligible (see Fig. 3). In fact, the strong dependence on the laser spot diameter indicates diffusion of electrons out of the laser spot which is equivalent to time of flight broadening. Figure 4 depicts the measured spin decay rate in dependence on the defocusing distance z which is the distance between the focus of the Gaussian laser beam and the sample. The squares show γ_z measured at 815 nm where BAP cannot be neglected and the circles show γ_z measured at 816 nm where BAP is unimportant. Measurements at 816 nm with twice the laser power (triangles) rule out that the observations can be attributed to excitation density dependent spin dephasing mechanisms as BAP. To model this time of flight broadening, we extend the existing spin noise model [9] by taking into account the classical position of the electron within the laser beam:

$$S(\omega) = \int d\mathbf{r}_0 \left| \mathcal{F}\left\{ \int d\mathbf{r} \exp(-\gamma_z^{\text{intr}} t) P(\mathbf{r}, \mathbf{r}_0) I(\mathbf{r}) \right\} \right|^2. \quad (2)$$

Here, the two-dimensional vector $\mathbf{r}_0$ gives the position of an individual electron at the beginning of the measurement, $\exp(-\gamma_z^{\text{intr}} t)$ describes the intrinsic spin decay, $I(\mathbf{r}) = I_0 \exp(-2r^2/w(z)^2)$ weights the position of the electron in the laser spot, and $P(\mathbf{r}, \mathbf{r}_0)$ gives the probability distribution for classical Brownian motion in two dimensions
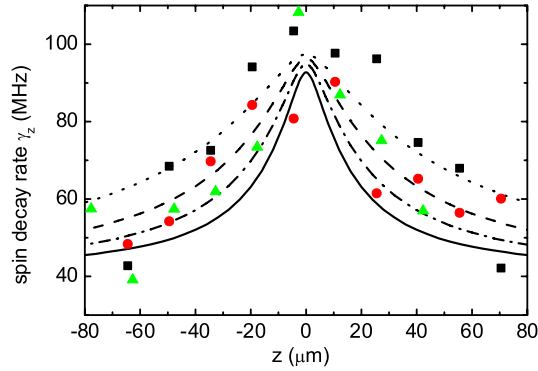
FIG. 4 (color online). Effective spin decay rate $\gamma_z = 1/\tau_z$ ($T = 20$ K) as a function of sample position z for a laser wavelength of $\lambda = 815$ nm (squares), $\lambda = 816$ nm (circles) and $\lambda = 816$ nm with doubled laser power (triangles). The $z = 0$ position is set to the maxima of the measured curves. The lines show calculations according to the model given by Eq. (2) for $D = 100$ cm^2/s (solid line), 200 cm^2/s (dash-dotted line), 400 cm^2/s (dashed line) and 1000 cm^2/s (dotted line).

with respect to a diffusion constant D [15]: $P(\mathbf{r}, \mathbf{r}_0) = 1/4\pi Dt \exp(-(\mathbf{r} - \mathbf{r}_0)^2/4Dt)$. The dependence of the effective spin decay rate on the sample position z is calculated numerically with Eq. (2) and is plotted in Fig. 4 for different values of D. The experimentally determined beam parameters are: waist $w_0 = 3.5$ μm and Rayleigh range $z_R = 3$ μm. As intrinsic spin decay rate, we determine $\gamma_z^{\mathrm{intr}} = 42(2.5)$ MHz. This value is the average decay rate to which the measured values converge when strongly defocused ($T = 20$ K and $\lambda = 815$ nm) and corresponds to a spin lifetime of $\tau_z^{\mathrm{intr}} = 24(2)$ ns which is to our knowledge the longest measured spin lifetime in n-doped GaAs (110) QWs. Best agreement between model and experiment is obtained for values of D between 100 and 1000 cm^2/s (see Fig. 4). The measured mobility at low temperature under illumination of $\mu = 3.7 \times 10^5$ cm^2/Vs gives together with the Einstein relation $D = \frac{\mu E_F}{e} \approx 2400$ cm^2/s ($E_F = 6.4$ meV). Contrary to electrical mobility measurements, in our experiment the electronic system has vanishing total momentum. Therefore, the Brownian motion within the laser spot is governed by electron-electron collisions that keep the total momentum of the electronic system constant and only represent a slight modification to the electrical conductivity that is mainly determined by electron-phonon and electron-impurity collisions. The electron-electron scattering time in thermal equilibrium calculates to $\tau_{ee} = 1/\{[\frac{\pi}{2}(k_B T)^2/\hbar E_F] \times \ln(E_F/k_B T)\} \approx 700$ fs for our sample system [16,17]. Calculating a diffusion constant from the Einstein relation together with the Drude model gives $D = 118$ cm^2/s. Thus, this coarse estimate yields an effective diffusion constant of the correct order of magnitude and shows that the experiment is sensitive enough to study electron motion near thermal equilibrium.

We attribute the residual intrinsic spin dephasing rate of $\gamma_z^{\mathrm{intr}} = 42(2.5)$ MHz to the DP mechanism due to random

Rashba fields caused by a fluctuating donor density in the symmetric doping layers [18]. The relevant area on which these donor density fluctuations between the layers have to be considered is given by $A = \pi(v_F \tau_{ee})^2$. Assuming a Poisson distribution, the donor fluctuations are of the order of $1/\sqrt{An} \approx 11\%$. The resulting electric field is calculated in a simple parallel-plate capacitor model. With the Rashba coefficient and Eq. (3) of Ref. [19] modified for the case of a degenerate electron gas, we obtain a spin dephasing rate of 10 MHz, which compares well to the measured rates in view of the approximations made.

In conclusion, we have shown that SNS allows to measure intrinsic spin lifetimes in n-doped GaAs (110) QWs. These lifetimes are limited by intrinsic, random Rashba fields that stem from unavoidable fluctuations in the donor density. Furthermore, we have shown that the spin noise spectra are time of flight broadened and theoretically described by a model which predicts that spin noise spectroscopy allows to study near equilibrium electron dynamics. Therefore, at millikelvin temperatures, which are generally accessible due to the nonperturbative nature of spin noise spectroscopy, modifications to the classical motion like weak localization effects [15] should become directly accessible at thermal equilibrium.

*mueller@nano.uni-hannover.de
[1] M. I. D'yakonov and V. I. Perel', Sov. Phys. Solid State **13**, 3023 (1972).
[2] G. Dresselhaus, Phys. Rev. **100**, 580 (1955).
[3] R. Winkler, Phys. Rev. B **69**, 045317 (2004).
[4] Y. Ohno et al., Phys. Rev. Lett. **83**, 4196 (1999).
[5] S. Döhrmann et al., Phys. Rev. Lett. **93**, 147405 (2004).
[6] O. D. D. Couto, Jr. et al., Phys. Rev. Lett. **98**, 036603 (2007).
[7] S. A. Crooker et al., Nature (London) **431**, 49 (2004).
[8] M. Oestreich et al., Phys. Rev. Lett. **95**, 216603 (2005).
[9] M. Römer, J. Hübner, and M. Oestreich, Rev. Sci. Instrum. **78**, 103903 (2007).
[10] M. Braun and J. König, Phys. Rev. B **75**, 085310 (2007).
[11] V. V. Bel'kov et al., Phys. Rev. Lett. **100**, 176806 (2008).
[12] E. Yablonovitch et al., Appl. Phys. Lett. **56**, 2419 (1990).
[13] S. Pfalz et al., Phys. Rev. B **71**, 165305 (2005).
[14] The optical absorption constant is adjusted so that measured and calculated spin noise power match at 815 nm and 20 K. Nonetheless, the value of α_0 is in good agreement with the literature (see, e.g., Ref. [13]).
[15] G. Bergmann, Phys. Rev. B **28**, 2914 (1983).
[16] G. Fasol, Appl. Phys. Lett. **59**, 2430 (1991).
[17] H. Fukuyama and E. Abrahams, Phys. Rev. B **27**, 5976 (1983).
[18] E. Y. Sherman, Appl. Phys. Lett. **82**, 209 (2003).
[19] P. S. Eldridge et al., Phys. Rev. B **77**, 125344 (2008).